

Received January 27, 2017, accepted February 15, 2017, date of publication March 1, 2017, date of current version May 17, 2017.

Digital Object Identifier 10.1109/ACCESS.2017.2675538

A Wearable Device and System for Movement and Biometric Data Acquisition for Sports Applications

MARKO KOS AND IZTOK KRAMBERGER, (Member, IEEE)

Faculty of Electrical Engineering and Computer science, University of Maribor, Maribor 2000, Slovenia.

Corresponding author: Marko Kos (marko.kos@um.si)

ABSTRACT This paper presents a miniature wearable device and a system for detecting and recording the movement and biometric information of a user during sport activities. The wearable device is designed to be worn on a wrist and can monitor skin temperature and pulse rate. Furthermore, it can monitor arm movement and detect gestures using inertial measurement unit. The device can be used for various professional and amateur sport applications and for health monitoring. Because of its small size and minimum weight, it is especially appropriate for swing-based sports like tennis or golf, where any additional weight on the arms would most likely disturb the player and have some influence on the player's performance. Basic signal processing is performed directly on the wearable device but for more complex signal analysis, the data can be uploaded via the Internet to a cloud service, where it can be processed by a dedicated application. The device is powered by a lightweight miniature LiPo battery and has about 6 h of autonomy at maximum performance.

INDEX TERMS Biometric data acquisition, inertial sensing, movement detection, pulse rate, sensor fusion, wearable.

I. INTRODUCTION

The cost of microelectromechanical systems (MEMS) has dropped dramatically due to the ever-growing popularity of smart wearable devices and smartphones. It is no surprise that the use of such smart devices has increased for sport activities and biometric monitoring applications. Wearable technology has been in use by businesses, medical professionals and military forces for decades, but the private consumer market for smart wearables has started to grow only recently. According to some forecasts, it is estimated that the market for smart wearables will rise up to \$5.8 billion by 2018 [1]. The most valuable segment of smart wearables are smart watches, taking 60% of the market value, followed by fitness and health trackers, smart jewelry and smart fashion. Many of smart wearable solutions come from young, crowd-funded startups, competing with the multinational electronic companies for their place in the smart wearables success story.

Smart wearables have found their place in many different applications and for many different tasks. In sports like golf, tennis, baseball, basketball, boxing, soccer, swimming, rowing, etc., they can be used for athlete's performance monitoring. Measuring and tracking performance and

biometric data usually includes many metrics, like acceleration, angular speed, temperature, pulse rate, etc. Smart wearables are also gaining popularity for health monitoring [2], clinical testing, human-machine interaction (HMI), where brain computer interfaces (BCI) are also gaining popularity [3]–[6], and even for educational support [7]. Beside MEMS-based approaches video and multimodal interaction is also often used for HMI and similar applications [8], [9].

Miniaturization of sensors, and low power wireless communication technologies have enabled engineers to design small and non-intrusive wearable devices that can be worn on a wrist, in a shoe, or are integrated into the sport equipment. For example, such devices are used to monitor linear and angular head accelerations in football to detect possible hazardous head impacts. The device is mounted inside the helmet and it tracks the frequency and severity of helmet impacts [10], [11]. For Baseball and softball, a swing tracker device was developed for monitoring different swing metrics, like power, speed and hitting zone [10].

For boxing several systems were developed to provide punch analysis and punch type statistics. Usually a small

device is fitted into the boxing glove and a small microprocessor analyses the accelerometer data to detect and distinguish between different punches [12]. Smart sensor devices were also proposed for soccer and basketball. A system for shot/pass classification during a soccer match using an inertial sensor-based approach was presented by Schuldhause *et al.* [13]. For basketball a system for counting shots made and shots missed using a double sensor-node approach was introduced. One sensor is located on the wrist and it captures each shot attempt, while a sensor located on a net registers if a shot was made or missed [10].

Although many amateur and professional athletes use smart wearables on a daily basis, the majority of the sport leagues still hold back on approving the devices for in-game use. There is also a safety factor, and some players/athletes are concerned about privacy issues. One of the first Sport Federations, which opened up to the use of smart wearables, was the International Tennis Federation (ITF). As of January 1, 2014, tennis players are not only allowed to wear sensors on their bodies, but they can also review critical information during set breaks [14]. Major League Baseball is also one of the first sport leagues that have approved wearable biometric devices for use during the game. So far players are allowed to wear a biometric baseball sleeve and a body-harness for pitching arm strain and movement tracking [15].

II. RELATED WORK

The way in which the proposed system is designed and the way it performs, it is especially suitable for golf or tennis. Although several systems and devices are available commercially, they usually support only stroke/swing classification and metrics, or they support only fitness tracking metrics, like steps, calories, heart-rate, etc. Wearable device that we are presenting supports tennis stroke classification and heart-rate and temperature measurement simultaneously.

In the field of tennis stroke recognition there has been plenty of work done previously using a visual approach [16], [17]. For Grand Slams and other important tennis competitions, the ITF approved the use of a video system with several calibrated high-speed video cameras, stationed around the court, and computer software for video processing. The system is very expensive and can only be used on one court at a time [18]. For everyday use, other methods and principles are more appropriate, such as using an inertial measurement unit (IMU) with tennis match post-analysis software.

Similar to tennis, IMU-based systems were also proposed for other sports. Swing motion detection using an inertial sensor based portable instrument was proposed for golf [19]. The portable instrument consists of a microcontroller, a tri-axis accelerometer, a tri-axis gyroscope, and a Bluetooth wireless transmission module. Another system for golf putt analysis was presented by Jensen *et al.* [20]. The system consists of off-the-shelf components with a removable sensor. The main features are an automatic putt detection with machine

learning methods and a real-time parameter calculation in the club coordinate system.

For tennis several smart wearable solutions exist, that use four different integration principles: a.) The sensor is integrated in a tennis racquet handle; b.) The sensor is attached on tennis racquet strings (like a string vibration dampener); c.) The sensor is attached on the tennis racquet grip; d.) The sensor is attached to a tennis player's wrist. The first option is also the most expensive, because the player has to buy a special tennis racquet. The racket logs different strokes and also the nature of the strokes, which are then synchronized with the mobile device via Bluetooth. The system has 6 hours of autonomy with one battery charge. It uses accelerometer, gyroscope and piezoelectric sensors to detect the strokes [10].

A system for a player's full movement tracking during a tennis match was proposed by L. Büthe *et al.* [21]. The system is composed of three inertial measurement units, one attached to each foot and one to the tennis racquet. A pipeline was developed to detect and classify leg and arm movement and implement gesture recognition for the shooting arm based on longest common subsequence (LCSS). The results showed that the shots are highly user-dependent. For stroke detection, the algorithm achieved 87% recall and 89% precision, whereas for step recognition the algorithm was able to detect 76% of the steps with a classification accuracy of 95%.

R. Srivastava *et al.* proposed a method for efficient characterization of tennis shots and game analysis based on wearable sensors data [22]. They developed an engine used for self-learning and/or coach-assisted training for swing-based games like tennis and golf. A Dynamic Time Warping algorithm is used for shot classification (forehand, backhand, and serve). At the second classification level the Quaternion Dynamic Time Warping classification algorithm (QDTW) was used to distinguish between slice and non-slice shots.

Multi-sensor classification of tennis strokes was proposed by Connaghan *et al.* [23]. In their work tennis stroke recognition was investigated using a single IMU attached to a player's forearm during a competitive match. For classification a two-level classification approach was used. In the first step non-stroke events were filtered and in the second step stroke candidates were classified into serves, backhands and forehands. 90% classification accuracy was achieved when the sensor fusion approach was implemented (a combination of data from an accelerometer, gyroscope and magnetometer was used for classification).

Tennis stroke detection and classification can also be addressed as a hand-gesture recognition problem [24]. In this area of research the popular methods for gesture recognition are Hidden Markov Models (HMM) [25], Dynamic Time Warping (DTW), and their derivatives (like QDTW).

III. SYSTEM ARCHITECTURE

The proposed system for movement and biometric data acquisition combines movement tracking of an athlete, where sport performance can be observed, and sensing of biometric information, like temperature and Pulse Rate (PR) or even Pulse

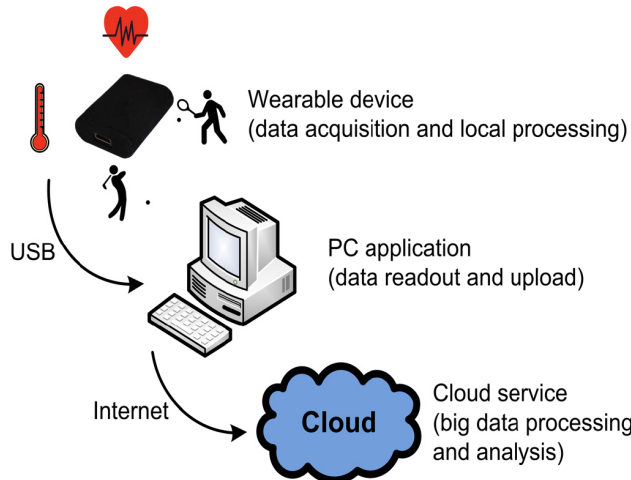


FIGURE 1. Architecture of the wearable device and system for movement and biometric data acquisition.

Rate Variability (PRV), from which additional information can be drawn about the physical and mental state. The design of the system is presented in Fig. 1.

The proposed system is composed of two main parts: 1) A miniature wearable device for movement and biometric information tracking, and 2) Cloud service for information visualization and detailed performance analysis. The wearable device tracks movement and gathers biometric information. Because the wearable device itself cannot connect directly to the cloud service, a computer or smart device with dedicated application is used to transfer data from the device and upload it to the cloud via the Internet, where more complex and sophisticated analyses can be performed. Further the cloud service enables extended collection of data from different locations and users and can provide support for big data oriented processing and statistics (e.g. as in [26]). In the following sections the individual segments of the system will be presented in detail.

A. WEARABLE DEVICE EMBEDDED HARDWARE DESIGN

The main goal of the system's hardware design was to design a light-weight motion and biometric information acquisition device that can be attached on the wrist of an athlete without influencing the player's performance. The optimum location for the device's position is right above the ulnar head. There is enough soft tissue between the ulna and the radius to measure PR and PRV successfully with the photo plethysmography (PPG) measuring technique during low-movement intervals. The position of the wearable device on the player's forearm and the orientation of the accelerometer axes are presented in Fig. 2. The gyroscope is oriented in such a way that when the accelerometer arrow is facing towards you, the angular rate is positive in counter-clockwise direction.

The device has to operate in a stand-alone manner while detecting and classifying basic strokes in real time. For more detailed stroke analysis sampling rate of the accelerometer and gyroscope data has to be high enough. According to some previous work regarding tennis racquet vibrations and string

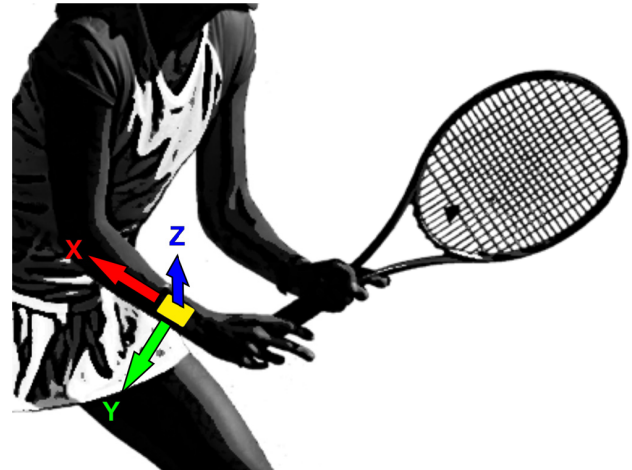


FIGURE 2. Wearable motion and biometric data acquisition device position and axes orientation. The device is attached on the player's hand right above the ulnar head.

oscillations we estimated, that sample rate of 1000 sps is enough [27]. This means that the memory storage has to be large enough to store individual strokes of an average tennis match. Tennis matches usually last around two hours. We can rarely see a match with duration of more than five hours (the longest tennis match record is held by J. Isner and N. Mahut of 11 hours and 5 minutes at 2010 Wimbledon Championships). During tennis match, the percentage of total playing time is around 23-30% on clay courts and 10-15% on fast court surfaces [28]. To achieve maximum battery autonomy and because of the higher data transfer rate we did not implement wireless connectivity, but used the USB connectivity instead. The USB connector is also used for battery charging. Block representation of the proposed wearable device's hardware is depicted in Fig. 3.

The physical implementation of the wearable device is presented in Fig. 4. The system is assembled on a 4-layer 1 mm thick FR4 Printed Circuit Board (PCB). The PCB measures 20 mm in width and 29.5 mm in length and with the battery attached it measures 7.2 mm in height. It weighs only 5.8 g and it can fit easily under a sweatband, which is often used by tennis players. The micro USB connector, micro- controller, battery charger, IMU unit, and FLASH memory are placed on the top layer, while the LED for pulse sensing, power supply, and the temperature sensor are placed on the bottom layer. The push button and the RGB LED are placed on the side of the device on the opposite side as the micro-USB connector. The main part of the motion and biometric data acquisition device is the high performance, low power 8/16-bit microcontroller with RISC architecture. It has 128 kB of FLASH program memory, 2 kB of EEPROM, and 8 kB of SRAM. It is running at 32 MHz clock from an internal calibrated clock source. It supports USB device interface, analog to digital conversion (ADC), SPI and I2C interfaces.

A MEMS IMU is used for sensing hand motion. It is composed of a tri-axis accelerometer and tri-axis gyroscope.

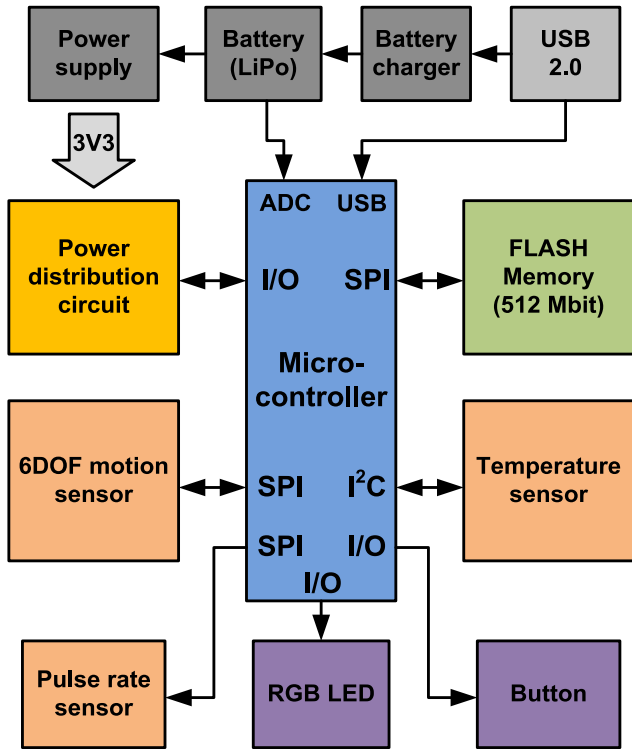


FIGURE 3. Block representation of the proposed wearable device embedded hardware. The heart of the system is a low-power 8/16-bit microcontroller.

Together they form 6 Degrees Of Freedom (DOF) device. The accelerometer measures linear acceleration with the measuring ranges of $\pm 2/\pm 4/\pm 8/\pm 16G$ and 16-bit resolution per axis. The gyroscope measures angular rate with the $\pm 125/\pm 245/\pm 500/\pm 1000/\pm 2000$ dps and 16-bit resolution per axis. It has an integrated FIFO memory of 8 kB, which enables the reading of data from the IMU device in burst mode, thus reducing the power consumption. An SPI interface is used for communication with the microcontroller. Maximum output data rate for the accelerometer is 6664 sps, and for the gyroscope 1666 sps. The device uses 0.9 mA in normal combo operational mode, and 1.2 mA in high-performance mode. High output data rates are available only in high-performance mode. The IMU unit is encapsulated in a LGA-16L package, measuring only $3 \times 3 \times 0.86$ mm, and is ideally suitable for our miniature design.

A pulse rate sensor with integrated analog front end is used for sensing the pulse of an athlete. The device consists of a low-noise receiver with an integrated ADC, an LED transmit section, and diagnostic circuit for sensor with LED fault detection. It uses an external 4 MHz clock source for precise clocking. As aforementioned, a PPG method for measuring an athlete's pulse rate is used. For illumination two pairs of LEDs with wavelengths of 880 nm and 660 nm are used. The principle of the PPG is that it measures the changes in volume, caused by the pressure pulse in the blood flow. Peripheral capillary oxygen saturation (or SpO₂) could also be measured because two different wavelengths for tissue illumination

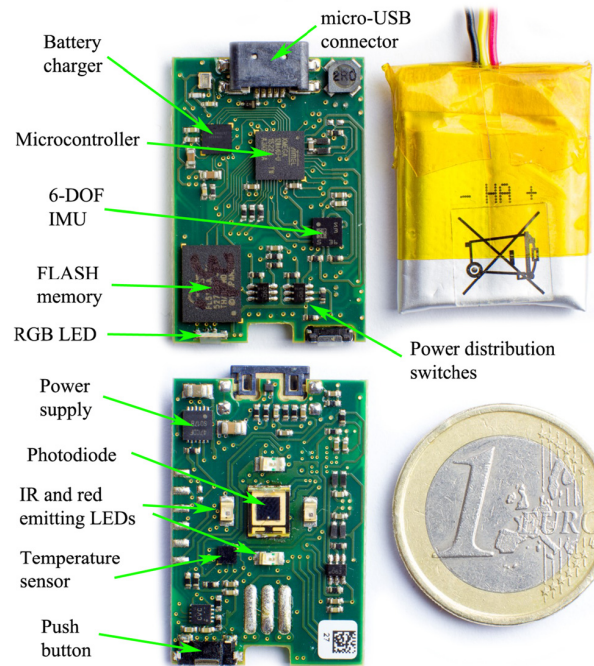


FIGURE 4. Physical implementation of the wearable device with individual sensor and sub-circuit position labels on the PCB.

are used. More information about the photo plethysmography method for pulse rate measurement and other applications can be found in [29] and [30]. High-speed and high-sensitivity silicon PIN photodiode receiver is used for the reflected light sensing. It has a large photo-sensitive area with the range of relative sensitivity from 430 nm to 1100 nm. The PIN photodiode operates in a zero bias mode because of the negative feedback from the input amplifier. The amplifier is a differential transimpedance amplifier and has a programmable gain in the range between 10 V/mA to 4×103 V/mA. The signal from the amplifier is sampled by a 22-bit ADC converter (sequentially for each LED wavelength) with a sample rate of 100 sps. The current for illumination LEDs can be set up to 100 mA with 8-bit resolution. The analog front-end is encapsulated in a compact DSBGA-36 package.

Contactless temperature sensing is implemented to sense the temperature of an athlete. It uses an infrared thermopile sensor with integrated math engine. It measures the temperature of an object by absorbing passive infrared energy at wavelengths between 4 μm to 16 μm . The internal math engine combines the corresponding change in voltage across the thermopile with the internal cold-junction reference temperature sensor to calculate the target object temperature. According to the manufacturer's documentation the sensor's accuracy in the temperature range between 0 °C to +65 °C is ± 1 °C max. The sensor also provides non-volatile memory for storing the calibration coefficients. The temperature readings are stored as 16-bit digital value. An I2C bus is used for communication with the microcontroller. Because rapid changes of the skin temperature of an athlete are not

expected, the temperature readings are made every 5 s. This sensor for temperature sensing was also selected because it has low power consumption. In normal operation mode the current consumption is $270 \mu\text{A}$ (typ.), and in shutdown mode the current consumption is $2 \mu\text{A}$ (max.). The temperature sensor is encapsulated in a miniature 8-pin DSBGA package thus taking up minimum space on the PCB.

An additional non-volatile flash memory is integrated in the system for storing the accelerometer and gyroscope data, the pulse-rate sensor data, the temperature sensor data, and timestamps of the samples. The capacity of the embedded memory is 512 Mbits. It uses an SPI bus to connect to the microcontroller. It can be used in Single Data Rate (SDR) or in Double Data Rate (DDR) mode. In both modes of operation the command bits are always latched on the rising edge of the clock. The difference between the two modes is that in the DDR mode the address and input data bits are latched on both the rising and falling edges of clock (SCK). The memory capacity can store approximately 1.5 hours of sport activities if continuous sampling mode is implemented. In stroke detection mode the memory can store approx. 8000 individual strokes, which can suffice for almost 6 hours of an average tennis match activity sampling (on average approx. 20 strokes per player per minute are taken into account [31]).

A push-button is implemented for powering up the device. The button is connected to the microcontroller via an interrupt input pin that can trigger the asynchronous interrupt. A long press is needed ($>1\text{s}$) to power up the device. The same logic is implemented for module power-down and transition into the stand-by (low power) mode. For simple device status indication RGB LED is integrated. When the system is in stand-by mode, the RGB LED is off. When the system is in active mode, the LED lights green. The red and blue colors are reserved for battery and memory status. When the battery is low, the red LED flashes for two seconds, and then the system goes to stand-by mode. If the red LED is lit continuously for five seconds, the memory of the device is full. The blue led is used to provide information about the charging cycle. During charging the blue LED flashes and when the battery is fully charged, the blue LED is lit continuously.

A USB connection is used to connect the device to a PC or smart device and to charge the Li-Po battery. A waterproof micro-USB type B connector is used for this purpose. A dedicated integrated circuit is used to charge the 155 mAh Li Po battery. The charger has a detection circuit for detecting the external power source (5 V typical). If a USB connection is detected, then the charging begins with 100 mA (low power USB port overload protection), otherwise setting for maximum allowed charging current is used. The charger has three phases of charging: 1) Pre-charge, 2) Fast-charge, and 3) Voltage regulation, to charge the battery to its full capacity. The maximum charge current ICHG can be programmed by an external resistor and is set to 155 mA. Charging is terminated when the charging current drops below the value of ICHG/10. During charging the circuit is monitoring the battery's

temperature for overheating protection. A safety timer is also integrated which terminates the charging procedure, if the battery's charging time exceeds the 10-hour limit.

A high-efficiency single-inductor buck boost DC/DC power supply is integrated for powering the system with appropriate voltage. The power is provided from the Li-Po battery, which can have the voltage from 4.2 V when fully charged, and around 3.0 V when almost fully discharged. Because a stable 3.3 V power supply voltage is required, a buck boost switch-mode power supply was chosen. The supply supports up to 1 A of output current and provide a stable output voltage over the complete input voltage range (2.7 V to 5.5 V) by switching automatically between buck or boost modes, depending on the input voltage. High switching frequency allows the use of tiny surface-mount components including a $2.2 \mu\text{H}$ inductor, a $10 \mu\text{F}$ input capacitor, and a $22 \mu\text{F}$ output capacitor.

Power switches are implemented to distribute the power to individual subsystems on the wearable device. P-type MOSFET transistors with low RDS(ON) resistance are used for this task. Power switches control the source of power for the 6 DOF IMU, the pulse rate sensor, the temperature sensor, and the FLASH memory. This mechanism is used to totally disconnect the individual parts of the circuit to achieve minimum current consumption.

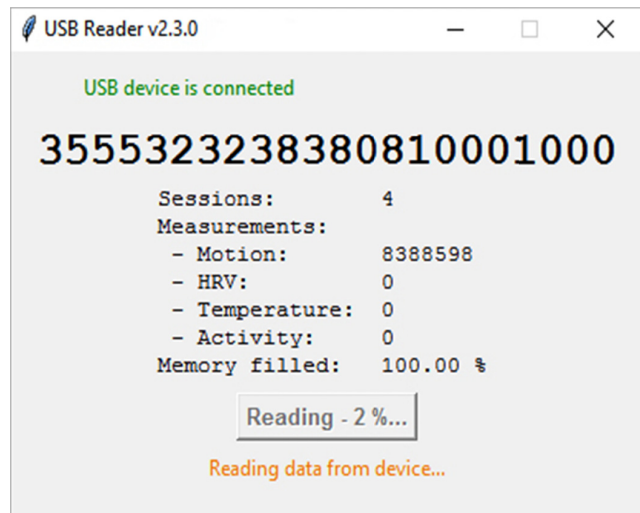


FIGURE 5. PC application graphical user interface. The application can read the wearable device, erase it, or update the firmware.

B. PC APPLICATION AND CLOUD SERVICE

The USB connection is, besides for charging the battery, also used for communication with the personal computer (PC) or portable device. When connected, the device is recognized as a generic HID device. On the PC side custom software is used to communicate with the wearable device. Software is used to download the data from the device and upload the information to the cloud service, to erase the device (empty the memory storage), and for firmware upgrades via USB. The graphical interface of the PC application is presented in Fig. 5.



FIGURE 6. Cloud service graphical web interface. The interface is used to visualize the uploaded motion and biometric information and also for in-depth game analyses.

After the motion and biometric data are uploaded to the cloud service, the uploaded information is visualized and ready for more detailed analysis. More sophisticated methods and statistical approaches can be used for a game and an athlete's game style analyses because more processing power and memory resources are available. The graphical web interface of the proposed cloud service is presented in Fig. 6.

IV. MOTION AND BIOMETRIC DATA ACQUISITION

This section covers the details regarding motion sensing and tracking, as well as biometric data acquisition. As mentioned before the system can be used for many different applications, but the design is especially suitable for swing-based sports like tennis or golf. Performance of the proposed system was tested with tennis players during competitive training. In the following sections the challenges of tennis stroke detection, tennis stroke classification and biometric data acquisition are addressed.

A. TENNIS STROKE DETECTION

For tennis stroke classification process individual tennis strokes first have to be detected accurately. We focused on detecting and classifying the three most common tennis strokes: Forehand, backhand, and serve.

By observing the accelerometer and gyroscope data in Fig. 7, one can see that, for every stroke, there are peaks in accelerometer readings in all three axes. The peaks are usually up to 10G in amplitude, but for serve, the acceleration peaks can reach up to 16G. To detect the strokes one could easily set up a threshold, and the stroke would be detected when the acceleration would surpass it. But the accelerometer readings can reach high values easily during the swings before the tennis ball even touches the racquet. By observing the accelerometer data more closely, one can see that at the point of impact, abrupt changes in the acceleration occur.

These changes are detected easily by calculating a two-point derivative of the acceleration curves. Because rotation normalization is not performed (i.e. different players hold the racket differently for the same type of stroke and

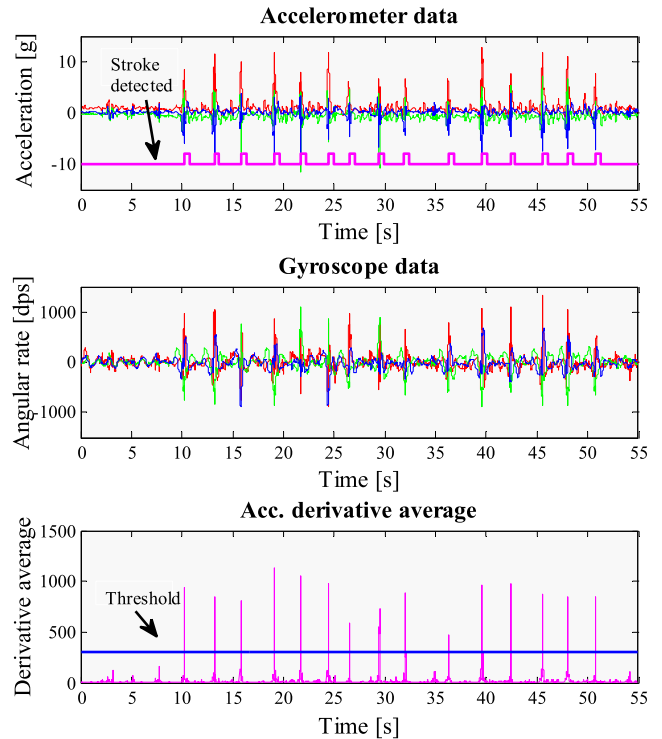


FIGURE 7. Graphical representation of the accelerometer and gyroscope data (x-axis = red, y-axis = green, z-axis = blue). The last sub-plot represents the average derivative of accelerometer data with a predefined threshold for tennis stroke detection.

as a consequence the angle of individual axis is therefore not always the same), the derivative average of the three accelerometer axes is calculated by the following expression:

$$D[n] = \frac{1}{3} \cdot \sum_{i=1}^3 |[A_i[n] - A_i[n-1]]|. \quad (1)$$

Where n is the sample data index, $D[n]$ is the average derivative value, and A_i is the acceleration sample for corresponding axis index i ($1 = X$ axis, $2 = Y$ axis, and $3 = Z$ axis). The stroke is detected when the average derivative $D[n]$ exceeds the predefined threshold. There are also other arm movements, which can trigger the stroke detection. In Fig. 7 on the accelerometer data plot small acceleration spikes can be noticed between 0-10 s. They are a result of the player picking up the ball with his racquet. It is also quite common that the players twirl their racquets whilst waiting on an opponent to serve [23]. It is not desirable to detect such events because they are not actual strokes and therefore an appropriate value of the derivative average threshold has to be determined. The threshold parameter of 300 was found to be suitable for reliable stroke detection across all 7 players considered in this study. By using an average acceleration derivative instead of actual acceleration average for detecting the stroke, the differences in the stroke force for different players do not represent a vital influence for accurate stroke detection.

B. TENNIS STROKE CLASSIFICATION

We addressed the problem of tennis stroke classification in our previous work [32]. The results in our previous work were preliminary and were achieved on a smaller database. We extended the database and modified the algorithm for tennis stroke classification. The Tennis Stroke Database (TSD) is composed of tennis stroke recordings with several different players with different levels of tennis knowledge (seniors, juniors, cadets). Seven players (6 right-handed, 1 left-handed) were recorded in different conditions (indoors, outdoors), different court surfaces (clay, hard surface), different tennis balls and racquets. The recordings are a mix of individual stroke sequences and competitive training with a mixture of strokes and game elements. 446 strokes were recorded overall. For easier TSD annotation, a video recording of each tennis player was made in parallel with the wearable device recordings. Recordings also include other types of tennis strokes (e.g. volleys, slices, smashes, etc.), which were not considered in the evaluation.

The basic idea behind the classification remains the same. Because accelerometer data alone does not provide enough discriminative features, gyroscope information for stroke classification is used. The algorithm looks for minimum and maximum values around the point of contact (this is the moment when tennis ball hits the racket) and determine in which axis they happen. The interval of observation for minimum and maximum tracking is 50 ms before the actual point of contact. The flowchart diagram of the tennis stroke classification principle is depicted in Fig. 8.

The stroke classification begins with IMU sensor sampling, where the accelerometer value derivative is being calculated constantly and compared with the predefined threshold (DTR). Gyroscope information of all three axes are sampled and buffered at the same time. For the purpose of classification 50 samples of gyroscope readings of each axis are being buffered. The sample buffer is located in the microcontroller's RAM. When the stroke is detected (acc. value derivative is higher than the DTR), the axis of minimum and maximum angular rate is searched in the sample buffer. If the maximum is found in the Y axis, the stroke is classified as a backhand. If the maximum corresponds to the X axis, and the minimum is found in the Z axis, the stroke is classified as a serve. If the maximum and minimum gyroscope values correspond to the X and Y axis accordingly, additional condition is checked of the minimum Z axis angular rate. If the angular rate is lower than 1500 dps the stroke is classified as a serve, otherwise the stroke is classified as a forehand. This condition was added to the classification algorithm because some tennis players tend to rotate the hand during the serve differently. If none of the above-mentioned combinations are true, the detected stroke is pronounced as unknown (UNKN.). Sometimes the players make the shots very close to the body or out of balance, and are therefore difficult to categorise as serve, forehand, and backhand. That is why we introduced the

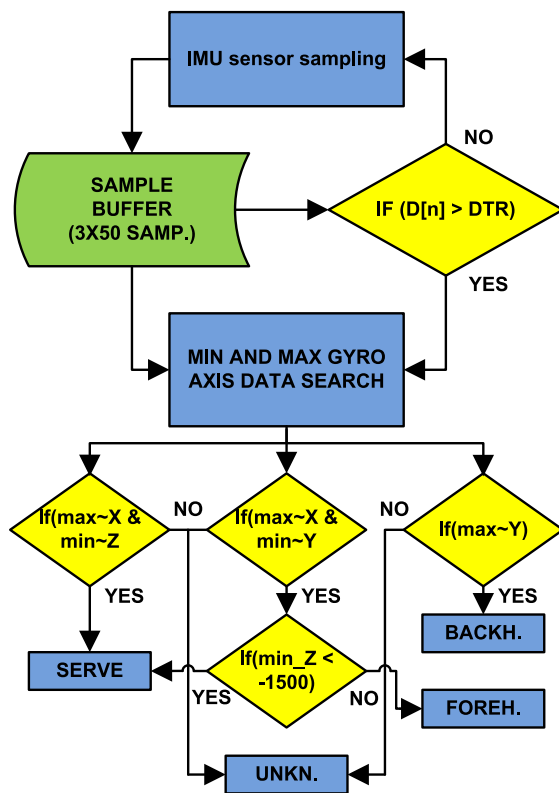


FIGURE 8. Flowchart diagram of the tennis stroke classification principle. Gyroscope data is used to discriminate between individual strokes.

unknown category. The embedded tennis stroke classification algorithm is executed on the microcontroller (in worst case) in 2385 clock cycles, which is 74.5 μ s at clock frequency of 32 MHz. The duration of the tennis stroke classification algorithm processing time was determined using the internal cycle counter of the microcontroller.

C. PULSE RATE AND PULSE RATE VARIABILITY

Pulse rate and pulse rate variability monitoring during the athlete's physical activity can give good insight about the athlete's mental and physical condition. The reflective photo plethysmography method is used for monitoring the pulse. For tissue illumination two different light sources are used (RED and IR LED). The photodiode is sampled with a sample rate of 100 Hz. Every heart beat is represented with a so-called R wave. Time between individual R waves is called the R-R interval. PR and PRV can be calculated by measuring this interval. Some PR and PRV experiments were performed in our previous work and the results are presented in [30]. The graphical representation of R-R intervals from RED and IR LED illumination are presented in Fig. 9. The PPG signal was obtained when the wrist was not moving (still position). The moments when the wrist is not moving are detected with readings from the IMU sensor.

D. TEMPERATURE MEASUREMENT

As mentioned before, a contactless thermopile temperature sensor is used for temperature measurement. The temperature

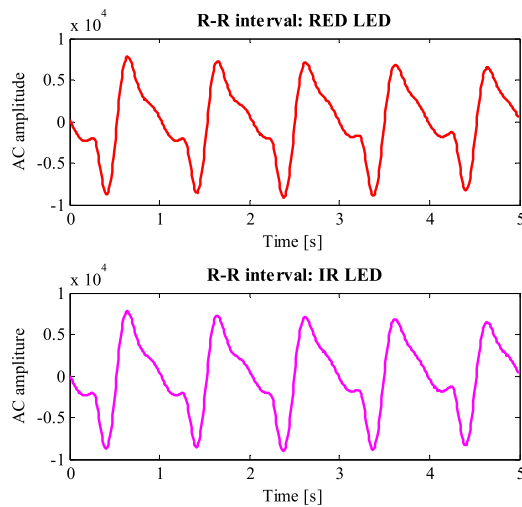


FIGURE 9. Graphical representation of R-R intervals obtained with the PPG method. The upper plot represents a signal obtained with red LED tissue illumination and the lower plot represents a signal obtained with IR LED tissue illumination.

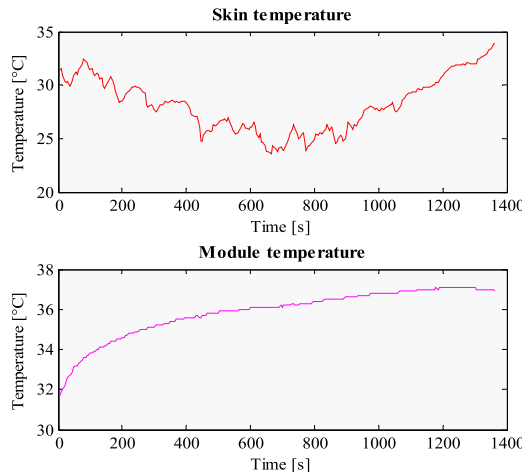


FIGURE 10. Temperature readings during a short (20 min) tennis practice. The upper plot represents readings of the skin temperature, while the lower plot represents the sensor's internal cold-junction temperature readings.

is estimated based on measuring the passive infrared energy of an object. For accurate temperature sensing the local (internal) temperature is measured (cold-junction temperature reference). This is necessary because thermopile sensors measure temperature differentials, not absolute temperature. A graphical representation of skin and device's temperature readings is presented in Fig. 10. For high precision temperature measurements the sensor has to be calibrated because of the different emissivity of different surfaces. We did not manage to perform that, therefore the temperature readings are currently not calibrated for skin readings.

We can notice from the plots in Fig. 10 that device's temperature was constantly rising during the practice. It has to be noted that the device was also slightly heating because of the LEDs for pulse rate measurement (the LEDs are positioned very close to the temperature sensor) and other circuits. This could be the reason that the device achieved a

temperature higher than 37°C . The skin temperature readings were changing constantly during the practice. The reasons for such temperature variations are: different levels of activity during the practice, sweating, short pauses, etc.

V. EXPERIMENTS AND RESULTS

A. POWER CONSUMPTION

Because the device for movement and biometrical data acquisition is battery powered, the power consumption is very important for maximum battery autonomy. During stand-by operation mode all the peripherals are shut down and only the microcontroller and switch mode power supply are operating. The power supply supports dual voltage operation and it is switched to 2.8 V output voltage for lower consumption. The dual output voltage mode can be switched easily via an input pin on the buck/boost circuit. When the device is in stand-by, the microcontroller is in power-save mode. In this mode all the clock sources are stopped, except the Real-Time Counter (RTC) is working. Current consumption of the device in stand-by mode is $160 \mu\text{A}$. With the 155 mAh Li-Po battery it can operate for over a month without recharging.

When the device is in working mode, all the needed peripherals and subsystems are powered on. During the high intensity movement the current consumption is around 20 mA, because the LEDs for PR monitoring are not active. When the movement is low and the LEDs are active, the current consumption rises to 33 mA. With the average current consumption of 25 mA the wearable device can operate over 6 hours with one battery charge. Because of the adaptive pulse-rate measurement principle the real current consumption depends on the player's activity. Current consumption in different modes was measured with a 6 1/2 digital μA -meter.

TABLE 1. Tennis stroke classification accuracy.

Stroke	Serve	Foreh.	Backh.	Unkn.	Acc. (%)
Serve	82	1	0	0	98.8
Foreh.	5	202	1	8	93.5
Backh.	1	0	144	1	98.6

B. TENNIS STROKE CLASSIFICATION ACCURACY

Tennis stroke classification accuracy evaluation was performed on an extended tennis stroke database. The database contains recordings of seven different tennis players with different tennis knowledge, which were recorded during competitive training sessions indoors and outdoors. The sessions took place on clay and hard court surfaces. Over 400 tennis strokes were evaluated. For stroke classification only information from gyroscope is used. The classification was performed with unsupervised method according to the algorithm presented in Fig. 8. Tennis stroke classification accuracy results are presented in Table 1.

The results from Table 1 show a relatively high stroke classification accuracy taking into account that the classification method is relatively simple. It presents a good basis for developing a more sophisticated method that would run

as a part of cloud service and would classify the strokes further into top-spin, flat and slice. It can also be noted that forehand has the lowest classification accuracy and when it is classified incorrectly, it is usually classified as unknown or as serve. The reason for this is because the forehand is the most often used stroke. The players use this type of stroke also in difficult positions (e.g. close to the body). Authors in [23] also performed tennis stroke classification accuracy for the three basic tennis strokes: forehand, backhand, and serve. Their approach was based on readings of IMU unit positioned on the player's forearm (accelerometer, gyroscope, and magnetometer). Tennis stroke detection was performed using accelerometer data, where tennis stroke candidates were first evaluated and appropriate candidates were then classified. For both steps naive Bayesian classifier was used. They trained the classifiers with the strokes of 4 and 7 players and tested on the unseen player. The best average tennis stroke accuracy of 90% was achieved when sensor fusion approach was used. We can say that our unsupervised method performs well comparing to the supervised approach proposed in [23].

C. PULSE-RATE AND PULSE-RATE VARIABILITY ACCURACY

To evaluate the wearable device's PR and PRV accuracy, three test subject were asked to participate in the test. The results of PR and PRV were compared with a calibrated PRV measuring device Biopac MP 36. For the wearable device signals obtained with red LED and with IR LED were evaluated. The results were calculated with the Kubios HRV analysis tool, which supports several input data formats for electrocardiogram (ECG) and R-R interval data [33]. Measurements were stored into the device's internal memory and were later downloaded and parsed into appropriate format. During measurement the test subjects were in a sitting position and the wearable device was attached to their wrist as presented in Fig. 2. Each measurement session lasted 10 min. One of the ways to present the variability of the PR is the standard deviation of the instantaneous pulse-rate values [33], labelled as STD PR in the table. This measure represents the short-term and long-term variations within the R-R interval series. The results of average pulse-rate (PR) and pulse-rate standard deviation (STD PR) are presented in Table 2.

TABLE 2. Pulse-rate (PR) and pulse-rate standard deviation (STD PR) results.

Test subject	Reference device		Wearable device			
	PR [1/min]	STD PR [1/min]	PR [1/min]	STD PR [1/min]	PR rel. err. [%]	Δ STD PR [1/min]
TS A, IR	57.5	2.1	57.8	3.4	0.6	1.3
TS A, red			59.7	4.2	3.9	2.1
TS B, IR	68.2	2.7	66.6	2.9	2.3	0.2
TS B, red			66.4	2.8	2.6	0.1
TS C, IR	71.2	3.2	70.9	3.4	0.5	0.2
TS C, red			71.5	3.3	0.4	0.1

The results in Table 2 show good performance of the wearable device compared to the reference device. If the signal obtained with the wearable device is good (the receiving

diode gets good reflection from the tissue), as in case of the test subject C, the error for PR and PRV is very low. In some cases the reflection can be poor due to the thick skin and the lack of larger blood vessels in the illuminated tissue. The sampling frequency of the reflection signal also influences the accuracy of PRV measurement. In our case the sampling frequency of wearable device was 100 sps, whereas the sampling frequency of the reference device was 1000 sps.

D. SKIN TEMPERATURE MEASUREMENT ACCURACY

To determine the accuracy of the proposed skin temperature measurement sensor, we measured skin temperature of 10 test subjects. This way the temperature measurement performance on different skin tones was evaluated. We compared the results of the proposed wearable device with a calibrated temperature measurement device Bosotherm diagnostic. The Bosotherm device has 0.1°C temperature resolution and $\pm 0.2^\circ\text{C}$ accuracy in the rage between 35°C and 42°C. During measurements the wearable device was attached on the wrist as presented in Fig. 2. The results obtained with this experiment are presented in Table 3.

TABLE 3. Skin temperature measurement accuracy.

Test subject	T _{SKIN} [°C] Bosotherm	T _{SKIN} [°C] Wearable	Absolute err. [°C]	Relative err. [%]
TS 1	35.8	35.85	0.05	0.14
TS 2	36.2	36.44	0.24	0.66
TS 3	36.0	35.98	0.02	0.06
TS 4	36.3	36.53	0.23	0.63
TS 5	35.6	35.54	0.06	0.17
TS 6	35.4	35.42	0.02	0.06
TS 7	36.3	36.31	0.01	0.03
TS 8	36.1	36.03	0.07	0.19
TS 9	36.1	36.03	0.07	0.19
TS 10	36.0	36.21	0.21	0.58
Average			0.1	0.27

As it can be seen from the results in Table 3, the wearable device is able to perform the human skin temperature measurement with minimum error (below 1%). The average absolute error is 0.1°C, and the maximum absolute error was only 0.24°C, which is basically just a bit above the Bosotherm device absolute accuracy threshold. From this we can conclude that the thermopile temperature sensor is appropriate for skin temperature measurement.

VI. CONCLUSION

This paper presents a wearable device and system for motion and biometric data acquisition that can be used for sports applications. The system is composed of a wearable device for data acquisition, and a cloud service for information visualization and more sophisticated game/athlete's performance analysis. Because of the wearable device's low weight and non-invasive methods for biometric information monitoring it is especially suitable for swing-based sports, like golf or tennis. The performance of the proposed system was tested for tennis, where tennis stroke classification performance for three different strokes was evaluated. The performance was tested on seven players with different levels of tennis

knowledge during a competitive training. The results show high classification accuracy and the proposed methods present a good basis for developing more sophisticated and accurate stroke classification and quality analysis algorithms in the future. Temperature measurement and pulse-rate detection also have good accuracy. Biometric data acquisition provides additional information about athlete's psychophysical condition and can contribute vital parameters for better in-depth game performance analysis.

ACKNOWLEDGMENT

The authors would like to thank the company Biometrika d.o.o. for their support.

REFERENCES

- [1] J. Wei, "How wearables intersect with the cloud and the Internet of Things: Considerations for the developers of wearables," *IEEE Trans. Consum. Electron.*, vol. 3, no. 3, pp. 53–56, Jul. 2014.
- [2] H. C. Chang, Y. L. Hsu, S. C. Yang, J. C. Lin, and Z. H. Wu, "A wearable inertial measurement system with complementary filter for gait analysis of patients with stroke or parkinson's disease," *IEEE Access*, vol. 4, pp. 8442–8453, Sep. 2016.
- [3] Y. Zhang, G. Zhou, J. Jin, X. Wang, and A. Cichocki, "Frequency recognition in SSVEP-based BCI using multisets canonical correlation analysis," *Int. J. Neural Syst.*, vol. 24, no. 4, pp. 1450013-1–1450013-14, 2014.
- [4] H. Wang *et al.*, "Discriminative feature extraction via multivariate linear regression for SSVEP-based BCI," *IEEE Trans. Neural Syst. Rehabil. Eng.*, vol. 24, no. 5, pp. 532–541, May 2016.
- [5] Y. Zhang, G. Zhou, J. Jin, Q. Zhao, X. Wang, and A. Cichocki, "Sparse Bayesian classification of EEG for brain-computer interface," *IEEE Trans. Neural Netw. Learn. Syst.*, vol. 27, no. 11, pp. 2256–2267, Nov. 2016.
- [6] Y. Zhang, Y. Wang, J. Jin, and X. Wang, "Sparse Bayesian learning for obtaining sparsity of EEG frequency bands based feature vectors in motor imagery classification," *Int. J. Neural Syst.*, vol. 27, no. 2, p. 1650032, 2017.
- [7] L. B. Chen, H. Y. Li, W. J. Chang, J. J. Tang, and K. S. M. Li, "WristEye: Wrist-wearable devices and a system for supporting elderly computer learners," *IEEE Access*, vol. 4, pp. 1454–1463, Apr. 2016.
- [8] Z. Lv, A. Halawani, S. Feng, H. Li, and S. U. Röhman, "Multimodal hand and foot gesture interaction for handheld devices," *ACM Trans. Multimed. Comput., Commun., Appl.*, vol. 11, no. 1, Sep. 2016.
- [9] Z. Lv, V. Penades, S. Blasco, J. Chirivella, and P. Gagliardo, "Evaluation of Kinect2 based balance measurement," *Neurocomputing*, vol. 208, pp. 290–298, Oct. 2016.
- [10] K. Lightman, "Silicon gets sporty," *IEEE Spectr.*, vol. 53, no. 3, pp. 48–53, Mar. 2016.
- [11] R. Jadischke, D. C. Viano, N. Dau, A. I. King, and J. McCarthy, "On the accuracy of the head impact telemetry (HIT) system used in football helmets," *J. Biomech.*, vol. 46, no. 13, pp. 2310–2315, Sep. 2013.
- [12] S. Chadli, N. Ababou, and A. Ababou, "A new instrument for punch analysis in boxing," *Procedia Eng.*, vol. 72, pp. 411–416, Jun. 2014.
- [13] D. Schuldhaus, C. Zwick, H. Koerger, E. Dorschky, R. Kirk, and B. Eskofier, "Inertial sensor-based approach for shot/pass classification during a soccer match," in *Proc. 21st ACM SIGKDD*, Sydney, Australia, Aug. 2015, pp. 1–4.
- [14] M. Zok, "Inertial sensors are changing the games," in *Proc. Int. Symp. Inertial Sensors Syst. (ISISS)*, Laguna Beach, CA, USA, Feb. 2014, pp. 1–3.
- [15] E. Waltz, "A wearable turns baseball pitching into a science," *IEEE Spectr.*, vol. 52, no. 9, pp. 16–17, Sep. 2015.
- [16] F. Yan *et al.*, "Automatic annotation of tennis games: An integration of audio, vision, and learning," *Image Vis. Comput.*, vol. 32, no. 11, pp. 896–903, Nov. 2014.
- [17] D. Connaghan, P. Kelly, and N. E. O'Connor, "Game, shot and match: Event-based indexing of tennis," in *Proc. 9th Int. Workshop Content-Based Multimedia Indexing (CBMI)*, Madrid, Spain, Jun. 2011, pp. 97–102.
- [18] N. Owens, C. Harris, and C. Stennett, "Hawk-eye tennis system," in *Proc. Int. Conf. Vis. Inf. Eng. (VIE)*, Jul. 2003, pp. 182–185.
- [19] Y. L. Hsu, Y. T. Chen, P. H. Chou, Y. C. Kou, Y. C. Chen, and H. Y. Su, "Golf swing motion detection using an inertial-sensor-based portable instrument," in *Proc. ICCE-TW*, Nantou, Taiwan, May 2016, pp. 1–2.
- [20] U. Jensen, M. Schmidt, M. Hennig, F. A. Dassler, T. Jaitner, and B. M. Eskofier, "An IMU-based mobile system for golf putt analysis," *Sports Eng.*, vol. 18, no. 2, pp. 123–133, 2015.
- [21] L. Büthe, U. Blanke, H. Capkevics, and G. Tröster, "A wearable sensing system for timing analysis in tennis," in *Proc. 13th Int. Conf. Wearable Implant. Body Sensor Netw. (BSN)*, San Francisco, CA, USA, Jun. 2016, pp. 43–48.
- [22] R. Srivastava, A. Patwari, S. Kumar, G. Mishra, L. Kaligounder, and P. Sinha, "Efficient characterization of tennis shots and game analysis using wearable sensors data," in *Proc. SENSORS*, Busan, South Korea, Nov. 2015, pp. 1–4.
- [23] D. Connaghan, P. Kelly, N. E. O'Connor, M. Gaffney, M. Walsh, and C. O'Mathuna, "Multi-sensor classification of tennis strokes," in *Proc. SENSORS*, Limerick, Republic of Ireland, Oct. 2011, pp. 1437–1440.
- [24] D. W. Lee, J. M. Lim, J. Sunwoo, I. Y. Cho, and C. H. Lee, "Actual remote control: A universal remote control using hand motions on a virtual menu," *IEEE Trans. Consum. Electron.*, vol. 55, no. 3, pp. 1439–1446, Aug. 2009.
- [25] D. Arsenault and A. D. Whitehead, "Gesture recognition using Markov Systems and wearable wireless inertial sensors," *IEEE Trans. Consum. Electron.*, vol. 61, no. 4, pp. 429–437, Nov. 2015.
- [26] Z. Lv, J. Chirivella, and P. Gagliardo, "Bigdata oriented multimedia mobile health applications," *J. Med. Syst.*, vol. 40, no. 5, pp. 1–10, May 2016.
- [27] F.-X. Li, D. Fewtrell, and M. Jenkins, "String vibration dampers do not reduce racket frame vibration transfer to the forearm," *J. Sport Sci.*, vol. 22, pp. 1041–1052, Nov. 2004.
- [28] J. Fernandez, A. Mendez-Villanueva, and B. M. Pluim, "Intensity of tennis match play," *Brit. J. Sports Med.*, vol. 40, no. 5, pp. 387–391, May 2006.
- [29] M. Elgendi, "On the analysis of fingertip photoplethysmogram signals," *Current Cardiol. Rev.*, vol. 8, no. 1, pp. 14–25, Feb. 2012.
- [30] J. Ženko, M. Kos, and I. Kramberger, "Pulse rate variability and blood oxidation content identification using miniature wearable wrist device," in *Proc. Int. Conf. Syst., Signal Image (IWSSIP)*, Bratislava, Slovakia, Jun. 2016, pp. 1–4.
- [31] S. Morante and J. Brotherhood, "Match characteristics of professional singles tennis," *J. Med. Sci. Tennis*, vol. 10, no. 3, pp. 12–13, Dec. 2005.
- [32] M. Kos, J. Ženko, D. Vlaj, and I. Kramberger, "Tennis stroke detection and classification using miniature wearable IMU device," in *Proc. Int. Conf. Syst., Signal Image (IWSSIP)*, Bratislava, Slovakia, Jun. 2016, pp. 1–4.
- [33] M. P. Tarvainen, J.-P. Niskanen, J. A. Lipponen, P. O. Ranta-aho, and P. A. Karjalainen, "Kubios HRV—Heart rate variability analysis software," *Comput. Methods Programs Biomed.*, vol. 113, no. 1, pp. 210–220, Jan. 2014.



MARKO KOS was born in 1981. He received the B.Sc. and Ph.D. degrees from the University of Maribor, Slovenia, in 2005 and 2010, respectively, all in electrical engineering. He is currently an Assistant and is a member of the Laboratory for Electronics and Information Systems, Faculty of Electrical Engineering and Computer Science. He has experience in embedded systems and hardware design. His research work extends into the fields of digital signal processing, embedded systems, and space technologies.



IZTOK KRAMBERGER (M'99) was born in 1973. He received the B.Sc., M.Sc., and Ph.D. degrees from the University of Maribor, Slovenia, in 1997, 2001, and 2003, respectively, all in electrical engineering. He has experience in embedded system design, programmable logic devices and electronic systems. Since 2009, he has been the Head of the Laboratory for Electronics and Information Systems, Faculty of Electrical Engineering and Computer Science, where he is currently an Assistant Professor. His research work extends into the fields of computer vision, brain-computer interfaces, and space technologies.